arXiv:cond-mat/0009442v1 [cond-mat.stat-mech] 28 Sep 2000

Density of a gas of spin polarized fermions in a magnetic field

S. Foulon, F. Brosens, J. T. Devreese*
Departement Natuurkunde, Universiteit Antwerpen (UIA), Universiteitsplein 1,
B-2610 Antwerpen

L. F. Lemmens
Departement Natuurkunde, Universiteit Antwerpen (RUCA),
Groenenborgerlaan171,
B-2020 Antwerpen

(To appear in Phys. Rev. E on December 1, 2000)

For a fermion gas with equally spaced energy levels that is subjected to a magnetic field, the particle density is calculated. The derivation is based on the path integral approach for identical particles, in combination with the inversion techniques for the generating function of the static response functions. Explicit results are presented for the ground state density as a function of the magnetic field with a number of particles ranging from 1 to 45.

I. INTRODUCTION

The explosive growth of mesoscopic physics in particular enabled to obtain a tunable number of electrons confined in semiconductor quantum dots [1]. Experiments on vertical quantum dots indicated that the confinement potential of single quantum dots is well described by a parabolic potential [2]. Although the electronic eigenstates and eigenvalues are essentially given by the Fock-Darwin states [3], detailed experimental data [4–6] reveal the importance of correlation effects on the ground state properties of the electrons in quantum dots. In order to take these correlation effects into account, various approximate theoretical methods [7–9] have been used. E.g., the eigenstates and eigenvalues of an harmonic interaction model including the effects of a magnetic field have been studied with operator techniques [10], and the harmonic interaction model has been used to explain specific features in the addition spectrum of a quantum dot in a magnetic field [11].

The harmonic interaction model is one of the rare examples for which the thermodynamical properties are exactly soluble, including the boson or fermion statistics, in the presence of a magnetic field [12]. It can also function as a trial model for the variational treatment of systems with more realistic interactions with the aid of the Jensen-Feynman inequality [13]. An example of this approach can be found in Ref. [14], where the Jensen-Feynman variational approach is used to describe the Bose-Einstein condensation in a gas of ^{87}Rb and in a gas of ^{7}Li atoms. The spin statistics of the harmonic interaction model [15] can be treated within the same many-body path integral formalism.

In the present paper, we study the density of harmonically interacting electrons in a parabolic quantum dot in a magnetic field, taking into account the electron correlation effects analytically. This analysis is a natural extension of our previous investigation of the thermodynamical properties of a confined system of spin-polarized fermions in the presence of a magnetic field [12], using a method that combines the path-integral formalism [16], the method of symmetrized density matrices [13], and inversion techniques for generating functions [17–19]. Instead of using the stochastic approach [20] with the Itô condition on the magnetic field [21] for calculating the path integral for N identical interacting oscillators in a magnetic field, we relied on a detailed investigation of the classical equations of motion. The quantum mechanical corrections to their classical action are exactly taken into account.

The model system of N harmonically interacting oscillators in a magnetic field is described by the Lagrangian (units with $\hbar$ and m equal to unity are used throughout this paper)

$$L = \frac{1}{2}\sum_{j=1}^{N}\left(\dot{\mathbf{r}}_j^2 - 2\omega_c x_j \dot{y}_j\right) - V, \tag{1}$$

---

[*] Also at Universiteit Antwerpen (RUCA), and at Technische Universiteit Eindhoven, NL 5600 MB Eindhoven, The Netherlands.

where ω_c is the cyclotron frequency, and where the potential energy V results from a harmonic confinement potential and a harmonic two-body interaction

$$V = \frac{\Omega^2}{2}\sum_{j=1}^{N}\mathbf{r}_j^2 \pm \frac{\omega^2}{4}\sum_{j,l=1}^{N}\left(\mathbf{r}_j - \mathbf{r}_l\right)^2 . \tag{2}$$

The two-body potential might be either attractive or repulsive depending on the plus sign or the minus sign in the two-body interaction.

As a first step in the calculation of the path integral, we studied the case of *distinguishable* particles [12]. Because the magnetic field only affects the equations of motion in the xy plane perpendicular to the magnetic field, the Lagrangian naturally decouples into two contributions $L = L_{xy} + L_z$, where L_{xy} contains the magnetic field. This allows to calculate the propagator in the xy-plane independently from the propagator in the z-direction. Through a transformation to the center of mass reference frame, one obtains a set of N three-dimensional oscillators in a magnetic field. The center of mass is described by an oscillator with frequency Ω. The remaining $N-1$ oscillators, associated with the internal degrees of freedom, have a frequency

$$w = \sqrt{\Omega^2 \pm N\omega^2}. \tag{3}$$

Note that the case of a repulsive interaction imposes a stability constraint on the confinement potential: Ω has to be large enough to keep the repelling particles together. The magnetic field does not affect these frequencies in the z direction. But in the xy plane the equations of motion reveal two renormalized frequencies due to the magnetic field

$$s = \sqrt{w^2 + \omega_L^2} \quad \text{and} \quad s_{c.m.} = \sqrt{\Omega^2 + \omega_L^2}, \tag{4}$$

where $\omega_L = \omega_c/2$ denotes the Larmor frequency. The index *c.m.* refers to the renormalized frequency in the center of mass coordinates.

Once the propagator for distinguishable particles is known, it is projected on the antisymmetric representation to obtain the *fermion* propagator [12].

This paper is organized as follows. In Sec. II the one-particle correlation function is calculated for identical harmonically interacting oscillators in a homogeneous magnetic field. In Sec. III special attention is paid to the fermion ground state density in the xy- and xz-plane. In section IV some concluding remarks are given.

II. STATIC RESPONSE PROPERTIES OF THE MODEL SYSTEM

In the path-integral approach to quantum mechanics the expectation value of a an expression $A\left(\bar{\mathbf{r}}\right)$ is given by

$$\left\langle A\left(\bar{\mathbf{r}},\beta\right)\right\rangle_I = \frac{\int d\mathbf{r}_1\cdots\int d\mathbf{r}_N K_I\left(\bar{\mathbf{r}},\beta\middle|\,\bar{\mathbf{r}},0\right)A\left(\bar{\mathbf{r}}\right)}{\int d\mathbf{r}_1\cdots\int d\mathbf{r}_N K_I\left(\bar{\mathbf{r}},\beta\middle|\,\bar{\mathbf{r}},0\right)}, \tag{5}$$

where $\bar{\mathbf{r}}$ is the $3N$-dimensional vector containing the coordinates $\mathbf{r}_1,\ldots,\mathbf{r}_N$ of all the N particles, and $K_I\left(\bar{\mathbf{r}},\beta\middle|\,\bar{\mathbf{r}}',0\right)$ denotes the propagator in the Euclidean time $\beta = 1/\left(k_B T\right)$, with k_B denoting the Boltzmann constant and T the temperature. The subscript I emphasizes that identical particles (fermions or bosons) are considered. For the probability density and its Fourier transform this gives

$$n\left(\mathbf{r}\right) = \frac{1}{N}\left\langle\sum_{l=1}^{N}\delta\left(\mathbf{r}-\mathbf{r}_l\right)\right\rangle_I = \int\frac{d\mathbf{q}}{\left(2\pi\right)^3}n_{\mathbf{q}}e^{-i\mathbf{q}\cdot\mathbf{r}} \longleftrightarrow n_{\mathbf{q}} = \frac{1}{N}\sum_{l=1}^{N}\left\langle e^{i\mathbf{q}\cdot\mathbf{r}_l}\right\rangle_I . \tag{6}$$

Substituting the expression for the propagator $K_I\left(\bar{\mathbf{r}},\beta\middle|\,\bar{\mathbf{r}},0\right)$, one obtains the following integral for the Fourier transform $n_{\mathbf{q}}$

$$\begin{aligned} n_{\mathbf{q}} = {} & \frac{1}{NZ_I\left(\beta,N\right)}\int\int\frac{d\mathbf{R}d\mathbf{k}}{\left(2\pi\right)^3}e^{i\mathbf{k}\cdot\mathbf{R}}\frac{K_\Omega\left(\sqrt{N}Z,\beta\middle|\,\sqrt{N}Z,0\right)K_{\omega_L,s_{c.m.}}\left(\sqrt{N}X,\sqrt{N}Y,\beta\middle|\,\sqrt{N}X,\sqrt{N}Y,0\right)}{K_w\left(\sqrt{N}Z,\beta\middle|\,\sqrt{N}Z,0\right)K_{\omega_L,s}\left(\sqrt{N}X,\sqrt{N}Y,\beta\middle|\,\sqrt{N}X,\sqrt{N}Y,0\right)} \\ & \times\int d\bar{\mathbf{r}}e^{-i\bar{\mathbf{k}}\cdot\bar{\mathbf{r}}}\sum_l e^{i\mathbf{q}\cdot\mathbf{r}_l}\frac{1}{N!}\sum_p\xi^p\prod_{j=1}^{N}K_w\left(\left(Pz\right)_j,\beta\middle|\,z_j,0\right)K_{\omega_L,s}\left(\left(Px\right)_j,\left(Py\right)_j,\beta\middle|\,x_j,y_j,0\right), \end{aligned} \tag{7}$$

where $Z_I(\beta, N) = \int d\bar{\mathbf{r}} K_I(\bar{\mathbf{r}}, \beta|\bar{\mathbf{r}}, 0)$ is the partition function of N identical particles, P denotes a permutation of the particle indices, and $\xi = +1$ for bosons and $\xi = -1$ for fermions. The propagators K_Ω, K_w, $K_{\omega_L, s_{c.m.}}$ and $K_{\omega_L,s}$ are known in closed form, and explicitly calculated in Ref. [12]. In order to obtain tractable expressions for $n_{\mathbf{q}}$, the summation over all possible permutations will be rewritten as a sum over all possible cycles.

A. One particle expectation values

For the one point correlation function a factor $e^{i\mathbf{q}\cdot\mathbf{r}_l}$ has to be taken into account in each permutation when applying the cyclic decomposition of the permutations. Indicating the number of cycles of length ℓ by M_ℓ, the cyclic decomposition for $n_{\mathbf{q}}$ becomes

$$n_{\mathbf{q}} = \frac{1}{NZ_I(\beta, N)} \int\int \frac{d\mathbf{R}d\mathbf{k}}{(2\pi)^3} e^{i\mathbf{k}\cdot\mathbf{R}} \frac{K_\Omega\left(\sqrt{N}Z, \beta\middle|\sqrt{N}Z, 0\right) K_{\omega_L, s_{c.m.}}\left(\sqrt{N}X, \sqrt{N}Y, \beta\middle|\sqrt{N}X, \sqrt{N}Y, 0\right)}{K_w\left(\sqrt{N}Z, \beta\middle|\sqrt{N}Z, 0\right) K_{\omega_L, s}\left(\sqrt{N}X, \sqrt{N}Y, \beta\middle|\sqrt{N}X, \sqrt{N}Y, 0\right)}$$
$$\times \sum_{M_1 \ldots M_N} \sum_\ell \ell M_\ell \mathcal{K}_\ell(\mathbf{k}, \mathbf{q}) \frac{\xi^{(\ell-1)M_\ell}}{M_\ell! \ell^{M_\ell}} \left(\mathcal{K}_\ell(\mathbf{k})\right)^{M_\ell - 1} \prod_{\ell' \neq \ell} \frac{\xi^{\left(\ell'-1\right)M_{\ell'}}}{M_{\ell'}! \left(\ell'\right)^{M_{\ell'}}} \left(\mathcal{K}_{\ell'}(\mathbf{k})\right)^{M_{\ell'}}, \tag{8}$$

with

$$\mathcal{K}_\ell(\mathbf{k}, \mathbf{q}) = \int d\mathbf{r}_{\ell+1} \ldots \int d\mathbf{r}_1 \delta(\mathbf{r}_{\ell+1} - \mathbf{r}_1) e^{i\mathbf{q}\cdot\mathbf{r}_1} \prod_{j=1}^{\ell} K_{\omega_L, s}(x_{j+1}, y_{j+1}, \beta| x_j, y_j, 0) K_w(z_{j+1}, \beta| z_j, 0) e^{-i\mathbf{k}\cdot\mathbf{r}_j/N}, \tag{9}$$

and $\mathcal{K}_\ell(\mathbf{k}, \mathbf{q} = 0) = \mathcal{K}_\ell(\mathbf{k})$ is the same function as Eq. (17) of Ref. [12] in the calculation of the partition function $Z_I(\beta, N)$. We point out that the positive integers ℓ and M_ℓ (with $1 \leq \ell \leq N$) have to satisfy the constraint $\sum_\ell \ell M_\ell = N$. Taking into account the semigroup property of the propagators $K_{\omega_L,s}(x_{j+1}, y_{j+1}, \beta \mid x_j, y_j, 0)$ and $K_w(z_{j+1}, \beta| z_j, 0)$, one recognizes in $\mathcal{K}_\ell(\mathbf{k}, \mathbf{q})$ the partition function (over a time interval $\ell\beta$) of a driven harmonic oscillator in a magnetic field

$$\mathcal{K}_\ell(\mathbf{k}, \mathbf{q}) = \int\int\int K_{\omega_L, s}(x, y, \ell\beta| x, y, 0) K_w(z, \ell\beta| z, 0) e^{-\int_0^{\ell\beta} \mathbf{f}_{\mathbf{q}}(\tau)\mathbf{r}(\tau)d\tau} dxdydz, \tag{10}$$

with the driving force

$$\mathbf{f}_{\mathbf{q}}(\tau) = i\frac{\mathbf{k}}{N} \sum_{j=0}^{\ell-1} \delta(\tau - j\beta) - i\mathbf{q}\delta(\tau). \tag{11}$$

This partition function is known in closed form and given by

$$\mathcal{K}_\ell(\mathbf{k}, \mathbf{q}) = \frac{1}{2(\cosh \ell\beta s - \cosh \ell\beta\omega_L)} \exp\left(\frac{\phi_{q_x, q_y}}{4s(\cosh \ell\beta s - \cosh \ell\beta\omega_L)}\right) \left(\frac{1}{2\sinh \frac{\ell\beta w}{2}} e^{\phi_{q_z}}\right), \tag{12}$$

with

$$\phi_{q_x, q_y} = \int_0^{\ell\beta}\int_0^{\ell\beta} \left(f_{q_x}(\tau) f_{q_x}(\sigma) + f_{q_y}(\tau) f_{q_y}(\sigma)\right) \begin{pmatrix} \cosh \omega_L(\tau - \sigma) \sinh s(\ell\beta - |\tau - \sigma|) \\ + \cosh \omega_L(\ell\beta - |\tau - \sigma|) \sinh s|\tau - \sigma| \end{pmatrix} d\sigma d\tau$$
$$+ i\int_0^{\ell\beta}\int_0^{\ell\beta} \left(f_{q_x}(\tau) f_{q_y}(\sigma) - f_{q_x}(\sigma) f_{q_y}(\tau)\right) \begin{pmatrix} \sinh \omega_L(\tau - \sigma) \sinh s(\ell\beta - |\sigma - \tau|) \\ - \sinh \omega_L(\ell\beta - |\sigma - \tau|) \sinh s(\tau - \sigma) \end{pmatrix} d\sigma d\tau, \tag{13}$$

$$\phi_{q_z} = \frac{1}{2}\int_0^{\ell\beta}\int_0^{\ell\beta} \frac{f_{q_z}(\tau) f_{q_z}(\sigma)}{2w} \frac{\cosh\left(\left(\frac{\ell\beta}{2} - |\tau - \sigma| w\right)\right)}{\sinh \frac{\ell\beta w}{2}} d\sigma d\tau. \tag{14}$$

Substituting the force $\mathbf{f}_{\mathbf{q}}(\tau)$ from (11) into the above expressions for ϕ_{q_x, q_y} and ϕ_{q_z} yields

$$\begin{aligned}\mathcal{K}_\ell\left(\mathbf{k},\mathbf{q}\right) &= \mathcal{K}_\ell\left(k_x,k_y\right)\exp\left(\frac{\left(k_xq_x+k_yq_y\right)\sinh\beta s}{2Ns\left(\cosh\beta s-\cosh\beta\omega_L\right)}-\frac{\left(q_x^2+q_y^2\right)\sinh\ell\beta s}{4s\left(\cosh\ell\beta s-\cosh\ell\beta\omega_L\right)}\right)\\ &\quad\times\mathcal{K}_\ell\left(k_z\right)\exp\left(\frac{k_zq_z}{2Nw}\coth\frac{1}{2}\beta w-\frac{q_z^2}{4w}\coth\frac{1}{2}\ell\beta w\right),\end{aligned}\tag{15}$$

with

$$\begin{aligned}\mathcal{K}_\ell\left(k_x,k_y\right) &= \frac{1}{2\left(\cosh\ell\beta s-\cosh\ell\beta\omega_L\right)}\exp\left(-\frac{\ell\left(k_x^2+k_y^2\right)}{4N^2s}\frac{\sinh\beta s}{\cosh\beta s-\cosh\beta\omega_L}\right),\\ \mathcal{K}_\ell\left(k_z\right) &= \frac{1}{2\left(\cosh\ell\beta w-1\right)}\exp\left(-\frac{\ell k_z^2}{4N^2w}\coth\frac{\beta w}{2}\right).\end{aligned}$$

The remaining integrations over $\mathbf{k}$ and $\mathbf{R}$ in $n_{\mathbf{q}}$ are Gaussian and easy to perform, eventually leading to

$$n_{\mathbf{q}}=\exp\left(\begin{array}{c}-\frac{\left(q_x^2+q_y^2\right)}{4N}\left(\frac{\sinh\beta s_{c.m.}}{s_{c.m.}\left(\cosh\beta s_{c.m.}-\cosh\beta\omega_L\right)}-\frac{\sinh\beta s}{s\left(\cosh\beta s-\cosh\beta\omega_L\right)}\right)\\ -\frac{q_z^2}{4N}\left(\frac{\coth\frac{\beta\Omega}{2}}{\Omega}-\frac{\coth\frac{\beta w}{2}}{w}\right)\end{array}\right)\tilde{n}_{\mathbf{q}},\tag{16}$$

with

$$\begin{aligned}\tilde{n}_{\mathbf{q}} &= \frac{1}{N\mathbb{Z}_I\left(\beta,N\right)}\sum_{M_1\ldots M_N}\left[\sum_\ell \ell M_\ell\exp\left(-\frac{\left(q_x^2+q_y^2\right)\sinh\ell\beta s}{4s\left(\cosh\ell\beta s-\cosh\ell\beta\omega_L\right)}-\frac{q_z^2}{4w}\coth\frac{1}{2}\ell\beta w\right)\right]\\ &\quad\times\prod_\ell\frac{\xi^{(\ell-1)M_\ell}}{M_\ell!\ell^{M_\ell}}\left(\frac{1}{4\left(\cosh\ell\beta s-\cosh\ell\beta\omega_L\right)\sinh\frac{1}{2}\ell\beta w}\right)^{M_\ell}.\end{aligned}\tag{17}$$

The exponential factor in $n_{\mathbf{q}}$ accounts for the center of mass contribution, and it becomes unity for non-interacting particles ($w=\Omega$). The factor $\tilde{n}_{\mathbf{q}}$ is the expectation value of $\sum_l e^{i\mathbf{q}\cdot\mathbf{r}_l}$ in the subspace of the relative coordinate system with its corresponding partition function $\mathbb{Z}_I\left(\beta,N\right)$.

We now introduce the generating function $\mathcal{G}_1\left(\beta,u,\mathbf{q}\right)=\sum_{N=0}^\infty\left(N\mathbb{Z}_I\left(\beta,N\right)\tilde{n}_{\mathbf{q}}\right)u^N$ for the Fourier transform of the density, as was done before [17,18] in the absence of a magnetic field,

$$\begin{aligned}\mathcal{G}_1\left(\beta,u,\mathbf{q}\right) &= \sum_{N=0}^\infty\sum_{M_1\ldots M_N}\left[\sum_\ell \ell M_\ell\exp\left(-\frac{\left(q_x^2+q_y^2\right)\sinh\ell\beta s}{8s\sinh\frac{\ell\beta}{2}\left(s+\omega_L\right)\sinh\frac{\ell\beta}{2}\left(s-\omega_L\right)}-\frac{q_z^2}{4w}\coth\frac{1}{2}\ell\beta w\right)\right]\\ &\quad\times\prod_\ell\frac{1}{M_\ell!}\left(\frac{\xi^{(\ell-1)}u^\ell}{\ell\left(8\sinh\frac{\ell\beta}{2}\left(s+\omega_L\right)\sinh\frac{\ell\beta}{2}\left(s-\omega_L\right)\sinh\frac{1}{2}\ell\beta w\right)}\right)^{M_\ell},\end{aligned}\tag{18}$$

$$=\Xi_I\left(\beta,u\right)\sum_{\ell=1}^\infty\frac{\xi^{(\ell-1)}\exp\left(-\frac{\left(q_x^2+q_y^2\right)\sinh\ell\beta s}{8s\sinh\frac{\ell\beta}{2}\left(s+\omega_L\right)\sinh\frac{\ell\beta}{2}\left(s-\omega_L\right)}-\frac{q_z^2}{4w}\coth\frac{1}{2}\ell\beta w\right)}{8\sinh\frac{\ell\beta}{2}\left(s+\omega_L\right)\sinh\frac{\ell\beta}{2}\left(s-\omega_L\right)\sinh\frac{1}{2}\ell\beta w}u^\ell,\tag{19}$$

where $\Xi_I\left(\beta,u\right)=\sum_{N=0}^\infty\mathbb{Z}_I\left(\beta,N\right)u^N$ is the generating function for the partition function $\mathbb{Z}_I\left(\beta,N\right)$. After straightforward algebra one is left with

$$\tilde{n}_{\mathbf{q}}=\frac{1}{N}\sum_{\ell=1}^N\xi^{(\ell-1)}\frac{\mathbb{Z}_I\left(\beta,N-\ell\right)}{\mathbb{Z}_I\left(\beta,N\right)}\frac{\exp\left(-\frac{\left(q_x^2+q_y^2\right)\sinh\ell\beta s}{8s\sinh\frac{\ell\beta}{2}\left(s+\omega_L\right)\sinh\frac{\ell\beta}{2}\left(s-\omega_L\right)}-\frac{q_z^2}{4w}\coth\frac{1}{2}\ell\beta w\right)}{8\sinh\frac{\ell\beta}{2}\left(s+\omega_L\right)\sinh\frac{\ell\beta}{2}\left(s-\omega_L\right)\sinh\frac{1}{2}\ell\beta w}.\tag{20}$$

It is noted that in the limit $\mathbf{q}\rightarrow 0$ the sum rule $\tilde{n}_{\mathbf{q}=0}=1$ is indeed satisfied. The density $n\left(\mathbf{r}\right)$ in real space then becomes

$$n\left(\mathbf{r}\right)=\int\frac{d\mathbf{q}}{\left(2\pi\right)^3}n_{\mathbf{q}}e^{-i\mathbf{q}\cdot\mathbf{r}}\tag{21}$$

$$=\frac{1}{N}\sum_{\ell=1}^N\xi^{(\ell-1)}\frac{\mathbb{Z}_I\left(\beta,N-\ell\right)}{\mathbb{Z}_I\left(\beta,N\right)}\frac{s\mathcal{B}_\ell}{\pi}\sqrt{\frac{w\mathcal{A}_\ell}{\pi}}\frac{\exp\left(-s\mathcal{B}_\ell\left(x^2+y^2\right)-w\mathcal{A}_\ell z^2\right)}{8\sinh\frac{\ell\beta}{2}\left(s+\omega_L\right)\sinh\frac{\ell\beta}{2}\left(s-\omega_L\right)\sinh\frac{1}{2}\ell\beta w},\tag{22}$$

with

$$\mathcal{A}_\ell = \left[\coth \frac{1}{2}\ell\beta w + \frac{1}{N}\left(\frac{w}{\Omega}\coth\frac{\beta\Omega}{2} - \coth\frac{\beta w}{2}\right)\right]^{-1}, \tag{23}$$

$$\mathcal{B}_\ell = \left[\frac{\sinh \ell\beta s}{\cosh \ell\beta s - \cosh \ell\beta\omega_L} + \frac{1}{N}\left(\frac{s}{s_{c.m.}}\frac{\sinh \beta s_{c.m.}}{\cosh \beta s_{c.m.} - \cosh \beta\omega_L} - \frac{\sinh \beta s}{\cosh \beta s - \cosh \beta\omega_L}\right)\right]^{-1}. \tag{24}$$

The sum rule $\int d\mathbf{r} n\left(\mathbf{r}\right) = 1$ for the density is easily verified. In the next subsection the fermion ground state density will be examined, by inverting the defining series for the generating function $\mathcal{G}_1\left(\beta, u, \mathbf{q}\right)$. Subsequently results will be presented for the ground state density in the xy-plane and in the xz-plane.

III. GROUND STATE DENSITY

Because of alternating signs in the recurrence relations for the partition functions $\mathbb{Z}_I\left(\beta, N\right)$, the equation (22) is not appropriate for numerical purposes, in particular in the low temperature limit. This sign problem can be circumvented by an alternative inversion of the generating function $\mathcal{G}_1$ using contour integration:

$$\tilde{n}_{\mathbf{q}} = \frac{1}{N!}\frac{1}{N\mathbb{Z}_I\left(\beta, N\right)}\left.\frac{\partial^N \mathcal{G}_1\left(\beta, u, \mathbf{q}\right)}{\partial u^N}\right|_{u=0} = \frac{1}{2\pi\mathbb{Z}_I\left(\beta, N\right)}\frac{1}{N}\int_0^{2\pi}\frac{\mathcal{G}_1\left(\beta, ue^{i\theta}, \mathbf{q}\right)}{u^N}e^{-iN\theta}d\theta. \tag{25}$$

Substituting (19) into the above expression yields

$$\begin{aligned}\tilde{n}_{\mathbf{q}} = {} & \frac{1}{N}\frac{\Xi_I\left(\beta, u\right)/u^N}{2\pi\mathbb{Z}_I\left(\beta, N\right)}e^{-\left(\kappa_x^2+\kappa_y^2+\kappa_z^2\right)} \\ & \times\sum_{\ell=1}^{\infty}\int_0^{2\pi}\frac{\Xi_I\left(\beta, ue^{i\theta}\right)}{\Xi_I\left(\beta, u\right)}\frac{\xi^{(\ell-1)}\left(\sqrt{bb_1b_2}ue^{i\theta}\right)^\ell \exp\left(-\left(\kappa_x^2+\kappa_y^2\right)\left(\frac{b_1^\ell}{1-b_1^\ell}+\frac{b_2^\ell}{1-b_2^\ell}\right)\right)\exp\left(-2\kappa_z^2\frac{b^\ell}{1-b^\ell}\right)}{\left(1-b^\ell\right)\left(1-b_1^\ell\right)\left(1-b_2^\ell\right)}e^{-iN\theta}d\theta,\end{aligned} \tag{26}$$

with the short hand notations

$$\kappa_x^2 = q_x^2/4s, \quad \kappa_y^2 = q_y^2/4s, \quad \kappa_z^2 = q_z^2/4w, \quad b = e^{-\beta w}, \quad b_1 = e^{-\beta(s+\omega_L)}, \quad b_2 = e^{-\beta(s-\omega_L)}. \tag{27}$$

By expanding the Fourier transform of the density $\tilde{n}_{\mathbf{q}}$ in powers of b, b_1 and b_2 one arrives at

$$\begin{aligned}\tilde{n}_{\mathbf{q}} = {} & \frac{1}{N}\frac{\Xi_I\left(\beta, u\right)}{2\pi\mathbb{Z}_I\left(\beta, N\right)u^N}e^{-\left(\kappa_x^2+\kappa_y^2+\kappa_z^2\right)}\sum_{m=0}^{\infty}\sum_{m_1=0}^{\infty}\sum_{n_1=0}^{\infty}\sum_{m_2=0}^{\infty}\sum_{n_2=0}^{\infty}\frac{\left(-\kappa_x^2\right)^{m_1+m_2}\left(-\kappa_y^2\right)^{n_1+n_2}\left(-2\kappa_z^2\right)^m}{\Gamma\left(m_1+1\right)\Gamma\left(m_2+1\right)\Gamma\left(n_1+1\right)\Gamma\left(n_2+1\right)\Gamma\left(m+1\right)} \\ & \times\sum_{k=0}^{\infty}\sum_{k_1=0}^{\infty}\sum_{k_2=0}^{\infty}\frac{\left(m_1+n_1+1\right)_{k_1}\left(m_2+n_2+1\right)_{k_2}\left(m+1\right)_k}{\Gamma\left(k_1+1\right)\Gamma\left(k_2+1\right)\Gamma\left(k+1\right)} \\ & \times\int_0^{2\pi}\frac{ue^{i\theta}b^{m+k+\frac{1}{2}}b_1^{k_1+m_1+n_1+\frac{1}{2}}b_2^{k_2+m_2+n_2+\frac{1}{2}}\Psi_{N-1}\left(\theta\right) - \xi\left(ub^{m+k+\frac{1}{2}}b_1^{k_1+m_1+n_1+\frac{1}{2}}b_2^{k_2+m_2+n_2+\frac{1}{2}}\right)^2\Psi_N\left(\theta\right)}{1-2\xi ub^{m+k+\frac{1}{2}}b_1^{k_1+m_1+n_1+\frac{1}{2}}b_2^{k_2+m_2+n_2+\frac{1}{2}}\cos\theta + \left(ub^{m+k+\frac{1}{2}}b_1^{k_1+m_1+n_1+\frac{1}{2}}b_2^{k_2+m_2+n_2+\frac{1}{2}}\right)^2}d\theta,\end{aligned} \tag{28}$$

with $\left(a\right)_p = \Gamma\left(a+p\right)/\Gamma\left(a\right)$ the Pochhammer symbol. The function $\Psi_N\left(\theta\right) = e^{-iN\theta}\Xi_I\left(\beta, ue^{i\theta}\right)/\Xi_I\left(\beta, u\right)$ has previously [12] been obtained. Using (6), the density (still at arbitrary temperature) then becomes

$$\begin{aligned}& n\left(\mathbf{r}\right) = \\ & \frac{1}{N}\frac{1}{\int_0^{2\pi}\Psi_N\left(\theta\right)d\theta}\sqrt{\frac{s^2w}{\pi^3A^2B}}\exp\left(-\frac{s\left(x^2+y^2\right)}{A}-\frac{wz^2}{B}\right) \\ & \times\sum_{m=0}^{\infty}\sum_{m_1=0}^{\infty}\sum_{n_1=0}^{\infty}\sum_{m_2=0}^{\infty}\sum_{n_2=0}^{\infty}\frac{\left(-\frac{1}{4A}\right)^{m_1+m_2+n_1+n_2}\left(-\frac{1}{2B}\right)^m}{\Gamma\left(m_1+1\right)\Gamma\left(m_2+1\right)\Gamma\left(n_1+1\right)\Gamma\left(n_2+1\right)\Gamma\left(m+1\right)}\end{aligned}$$

$$\times\sum_{k=0}^{\infty}\sum_{k_1=0}^{\infty}\sum_{k_2=0}^{\infty}\frac{\left(m_1+n_1+1\right)_{k_1}\left(m_2+n_2+1\right)_{k_2}\left(m+1\right)_k}{\Gamma\left(k_1+1\right)\Gamma\left(k_2+1\right)\Gamma\left(k+1\right)}$$

$$\times\sum_{q=0}^{m}\sum_{q_1=0}^{m_1+m_2}\sum_{q_2=0}^{n_1+n_2}\frac{\left(-\frac{4sx^2}{A}\right)^{m_1+m_2-q_1}\left(-\frac{4sy^2}{A}\right)^{n_1+n_2-q_2}\left(-\frac{4wz^2}{B}\right)^{m-q}}{\left(2\left(m_1+m_2\right)+1\right)_{-2q_1}\Gamma\left(q_1+1\right)\left(2\left(n_1+n_2\right)+1\right)_{-2q_2}\Gamma\left(q_2+1\right)\left(2m+1\right)_{-2q}\Gamma\left(q+1\right)}$$

$$\times\int_0^{2\pi}\frac{ue^{i\theta}b^{m+k+\frac{1}{2}}b_1^{k_1+m_1+n_1+\frac{1}{2}}b_2^{k_2+m_2+n_2+\frac{1}{2}}\Psi_{N-1}\left(\theta\right)-\xi\left(ub^{m+k+\frac{1}{2}}b_1^{k_1+m_1+n_1+\frac{1}{2}}b_2^{k_2+m_2+n_2+\frac{1}{2}}\right)^2\Psi_N\left(\theta\right)}{1-2\xi ub^{m+k+\frac{1}{2}}b_1^{k_1+m_1+n_1+\frac{1}{2}}b_2^{k_2+m_2+n_2+\frac{1}{2}}\cos\theta+\left(ub^{m+k+\frac{1}{2}}b_1^{k_1+m_1+n_1+\frac{1}{2}}b_2^{k_2+m_2+n_2+\frac{1}{2}}\right)^2}d\theta, \tag{29}$$

with

$$A=1+\frac{1}{N}\left(\frac{s}{s_{c.m.}}\frac{\sinh\beta s_{c.m.}}{\cosh\beta s_{c.m.}-\cosh\beta\omega_L}-\frac{\sinh\beta s}{\cosh\beta s-\cosh\beta\omega_L}\right), \tag{30}$$

$$B=1+\frac{1}{N}\left(\frac{w}{\Omega}\coth\frac{\beta\Omega}{2}-\coth\frac{\beta w}{2}\right). \tag{31}$$

The ground state density at $T=0$ is then readily obtained by taking the limit $\beta\to\infty$:

$$n_{T=0}\left(\mathbf{r}\right)$$

$$=\frac{1}{N}\sqrt{\frac{\left(\sigma s\right)^2\vartheta w}{\pi^3}}\exp\left(-\sigma s\left(x^2+y^2\right)-\vartheta wz^2\right) \tag{32}$$

$$\times\sum_{m=0}^{\infty}\sum_{m_1=0}^{\infty}\sum_{n_1=0}^{\infty}\sum_{m_2=0}^{\infty}\sum_{n_2=0}^{\infty}\frac{\left(-\frac{\sigma}{4}\right)^{m_1+m_2+n_1+n_2}\left(-\frac{\vartheta}{2}\right)^m}{\Gamma\left(m_1+1\right)\Gamma\left(m_2+1\right)\Gamma\left(n_1+1\right)\Gamma\left(n_2+1\right)\Gamma\left(m+1\right)}$$

$$\times\sum_{k=0}^{\infty}\sum_{k_1=0}^{\infty}\sum_{k_2=0}^{\infty}\frac{\left(m_1+n_1+1\right)_{k_1}\left(m_2+n_2+1\right)_{k_2}\left(m+1\right)_k}{\Gamma\left(k_1+1\right)\Gamma\left(k_2+1\right)\Gamma\left(k+1\right)}$$

$$\times\sum_{q=0}^{m}\sum_{q_1=0}^{m_1+m_2}\sum_{q_2=0}^{n_1+n_2}\frac{\left(-4\sigma sx^2\right)^{m_1+m_2-q_1}\left(-4\sigma sy^2\right)^{n_1+n_2-q_2}\left(-4\vartheta wz^2\right)^{m-q}}{\left(2\left(m_1+m_2\right)+1\right)_{-2q_1}\Gamma\left(q_1+1\right)\left(2\left(n_1+n_2\right)+1\right)_{-2q_2}\Gamma\left(q_2+1\right)\left(2m+1\right)_{-2q}\Gamma\left(q+1\right)}, \tag{33}$$

with

$$\sigma=\frac{N}{N-1+s/s_{c.m.}}\quad\text{and}\quad\vartheta=\frac{N}{N-1+w/\Omega}. \tag{34}$$

The sum rule $\int d\mathbf{r}n_{T=0}\left(\mathbf{r}\right)=1$ can easily be verified.

A. Density in the xy-plane

The ground state surface density $n(x,y)\equiv n_{T=0}\left(x,y,z\right)/n_{T=0}(0,0,z)$ in the xy plane is cylindrically symmetric, which means that $n(x=0,y)$ contains all the information. Figure 1 shows $Nn(x=0,y)/w$ for 1 up to 45 electrons for the non-interacting case ($w=\Omega$) at zero temperature. The factor $1/w$ makes this expression dimensionless (in the units with $\hbar=m=1$ used throughout this paper). The factor N is introduced for clarity in the figure, in order to avoid too strongly overlapping curves. The densities for $N=1$, 3, 6, 10, 15, 21, 28, 36, 45 electrons, i.e. for closed shell configurations, are emphasized by dashed lines. Oscillations appear in the density profiles, indicating concentric orbitals of increased density around the center of the confinement potential. The oscillations become more pronounced if the number of particles increases. Previously [22] the effects of an attractive ($w>\Omega$) and a repulsive ($w<\Omega$) two-particle interaction have been studied in the absence of a magnetic field. It was seen that a repulsive interaction induced an expansion whereas an attractive interaction induced a contraction of the gas of interacting fermions. These effects also appear for non-zero magnetic fields, but for brevity reasons they are not plotted.

With increasing magnetic field the oscillations in the density gradually become less pronounced and the confinement is enhanced as ω_L increases. The density profile changes whenever the magnetic susceptibility (which is proportional to $\partial E_G/\partial\omega_L$ with $E_G=\sum_{E<E_F}E$ the ground state energy) exhibits a discontinuity as a function of the magnetic field. For $\omega_L\gg w$ the energy spectrum behaves like a Landau spectrum. This is illustrated for the non-interacting case ($w=\Omega$) in fig. 2a and fig. 2b for $N=10$ electrons, and in fig. 3a and fig. 3b for $N=28$ electrons. The insets show the magnetic susceptibility as a function of ω_L.

B. Density in the xz-plane

Similarly as for the density in the xy-plane, the density profile in the xz-plane changes whenever there is a jump in the magnetic susceptibility. Figure 4 shows density contour plots for 4 fermions ($w = \Omega$) for various magnetic fields. The asymmetry of the x- and z-direction due to the magnetic field along the z-axis is clearly revealed in the plots. In fig. 5 the density contours for 10 fermions ($w = \Omega$) in the xz-plane are illustrated.

IV. CONCLUSION AND DISCUSSION

In this paper we have presented analytical results for the density of spin-polarized harmonically interacting fermion oscillators in a magnetic field, taking the fermion statistics of the particles into account. The approach presented here is valid for any number of electrons and for any temperature. We concentrated on the ground state density for a number of particles ranging from 1 up to 45, although also higher particle numbers can be treated. The density, in the xy- as well as in the xz-plane, shows a magnetic field dependency that is governed by the discontinuity in the magnetic susceptibility. Oscillations are present in the density and they are more pronounced as the number of particles is increased. These oscillations are smoothed out and finally disappear with increasing Larmor frequency ω_L. Whenever the magnetic field causes a discontinuity in the magnetic susceptibility, the density profile undergoes a sudden change, thus providing a means for characterizing the parameters of the system. To the best of our knowledge, the path integral approach used in this paper is the only method so far that provides this detailed information on the density for an interacting fermion system.

ACKNOWLEDGMENTS

Part of this work is performed in the framework of the FWO projects No. G.0287.95, 1.5.545.98, G.0071.98, and WO.073.94N [Wetenschappelijke Onderzoeksgemeenschap over “Laag-dimensionele systemen” (Scientific Research Community on Low-Dimensional Systems)], the “Interuniversitaire Attractiepolen – Belgische Staat, Diensten van de Eerste Minister – Wetenschappelijke, Technische en Culturele aangelegenheden” (Interuniversity Poles of Attraction Programs – Belgian State, Prime Minister’s Office – Federal Office for Scientific, Technical and Cultural Affairs), and in the framework of the GOA BOF UA 2000 projects of the Universiteit Antwerpen. The authors F. Brosens and S. Foulon acknowledge the FWO (Fonds voor Wetenschappelijk Onderzoek – Vlaanderen) for financial support.

---

[1] L. P. Kouwenhoven et al., *Electron transport in quantum dots in Proceedings of the Advanced Study Institute on Mesoscopic Electron Transport*, edited by L. L. Sohn, L. P. Kouwenhoven and G. Shön (Kluwer, Dordrecht, 1997).
[2] S. Tarucha, D. G. Austing, T. Honda, R. J. van der Hage, and L. P. Kouwenhoven, Phys. Rev. Lett. **77**, 3631 (1996).
[3] V. Fock, Z. Phys. **47**, 446 (1928); C. G. Darwin, Proc. Cambridge Philos. Soc. **27**, 86 (1930).
[4] R. C. Ashoori, Nature **379**, 413 (1996).
[5] N. B. Zhitenev, R. C. Ashoori, L. N. Pfeiffer, K. W. West, Phys. Rev. Lett. **79**, 2308 (1997)
[6] S. Tarucha, D. G. Austing, Y. Tokura, W. G. van der Wiel, and L. P. Kouwenhoven, Phys. Rev. Lett. **84**, 2485 (2000).
[7] M. Koskinen, M. Manninen, and S. M. Riemann, Phys. Rev. Lett. **79**, 1389 (1997).
[8] H.-M. Müller, and S. E. Koonin, Phys. Rev. B **54**, 14532 (1996).
[9] I.-H. Lee, V; Rao, R. M. Martin, and J.-P. Leburton, Phys. Rev. B **57**, 9035 (1998).
[10] N. F. Johnson en M.C. Payne, Phys. Rev. Lett. **67**, 1157 (1991).
[11] A. Angelucci and A. Tagliacozzo, Phys. Rev. B **50**, 7088 (1997).
[12] S. Foulon, F. Brosens, J. T. Devreese, and L. F. Lemmens, Phys. Rev. E **59**, (1999).
[13] R. P. Feynman, *Statistical Mechanics, a Set of Lectures*, W. A. Benjamin Inc., Reading, 1972.
[14] J. Tempere, F. Brosens, L. F. Lemmens, and J. T. Devreese, Phys. Rev. A **61**, 043605 (2000).
[15] L. F. Lemmens, F. Brosens, and J. T. Devreese, Phys. Rev. E **61**, 3358 (2000).
[16] R. P. Feynman and A. R. Hibbs, *Quantum Mechanics and Path Integrals*, Mc Graw Hill, New York, 1965.
[17] F. Brosens, J. T. Devreese, and L. F. Lemmens, Phys. Rev. E **55**, 227 (1997); **55**, 6795 (1997).
[18] F. Brosens, J. T. Devreese, and L. F. Lemmens, Phys. Rev. E **57**, 3871 (1998); **58**, 1634 (1998).
[19] L. F. Lemmens, F. Brosens, and J. T. Devreese, Solid State Commun. **109**, 615 (1999).

[20] B. Simon, *Functional Integration and Quantum Physics* (Academic, New York, 1979).
[21] L. S. Schulman, *Techniques and Applications of Path Integration* (Wiley, New York, 1979).
[22] J. Tempere, F. Brosens, L. F. Lemmens, and J. T. Devreese, Solid State Commun. **110**, 197 (1999).

Figure captions

Fig. 1: Scaled surface density $Nn\,(x=0,y)\,w$ for $\Omega = w$ in the plane perpendicular to the magnetic field, as a function of the scaled distance y/y_0 (with $y_0 = 1/\sqrt{w}$, units with $\hbar = m = 1$ are used) from the centre of the parabolic confinement potential for $N = 1, \ldots, 45$ fermions in the limit $\omega_L/w \to 0$. The densities corresponding to 1, 3, 6, 10, 15, 21, 28, 36, 45 fermions (i.e. for closed shell configurations in the absence of a magnetic field) are indicated by dashed lines and the corresponding particle number is explicitly indicated.

Fig. 2: **a**) Scaled surface density $Nn\,(x=0,y)\,/w$ for $\Omega = w$ in the plane perpendicular to the magnetic field, as a function of the scaled distance y/y_0 (with $y_0 = 1/\sqrt{w}$) from the centre of the parabolic confinement potential for $N = 10$ fermions and for various Larmor frequencies $\omega_L/w = 0.2$, 0.6, 1.2, 3.0. The inset shows the magnetic susceptibility for $N = 10$ fermions as a function of the Larmor frequency; **b**) Same as in Fig. 2a, but for $\omega_L/w = 0$, 0.4, 0.9.

Fig. 3: **a**) Scaled surface density $Nn\,(x=0,y)\,/w$ for $\Omega = w$ as a function of the scaled distance y/y_0 (with $y_0 = 1/\sqrt{w}$) from the centre of the parabolic confinement potential for $N = 28$ fermions and for various Larmor frequencies $\omega_L/w = 0$, 1.0, 2.0, 3.0. The inset shows the magnetic susceptibility for $N = 28$ fermions as a function of ω_L; **b)** Same as in Fig. 3a, but for $\omega_L/w = 0.5$, 1.5, 2.5, 3.5.

Fig. 4: Contourplots of $Nn\,(x,z)\,/w$ for $N = 4$ fermions and for $\Omega = w$ as a function of the scaled coordinates x/x_0 and z/z_0 with $x_0 = z_0 = 1/\sqrt{w}$, measured from the center of the parabolic confinement potential, for different values of the magnetic field: (a) $\omega_L/w = 0.2$, (b) $\omega_L/w = 1.0$, (c) $\omega_L/w = 1.5$, and (d) $\omega_L/w = 3.0$.

Fig. 5: Contourplots of $Nn\,(x,z)\,/w$ for $N = 10$ fermions and for $\Omega = w$ as a function of the scaled coordinates x/x_0 and z/z_0 with $x_0 = z_0 = 1/\sqrt{w}$, measured from the center of the parabolic confinement potential for different values of the magnetic field: (a) $\omega_L/w = 0.3$, (b) $\omega_L/w = 0.5$, (c) $\omega_L/w = 0.7$, (d) $\omega_L/w = 1.2$; (e) $\omega_L/w = 2.0$, (f) $\omega_L/w = 2.5$, (g) $\omega_L/w = 4.0$, (h) $\omega_L/w = 5.0$.

This figure "fig1.jpg" is available in "jpg" format from:

http://arXiv.org/ps/cond-mat/0009442v1

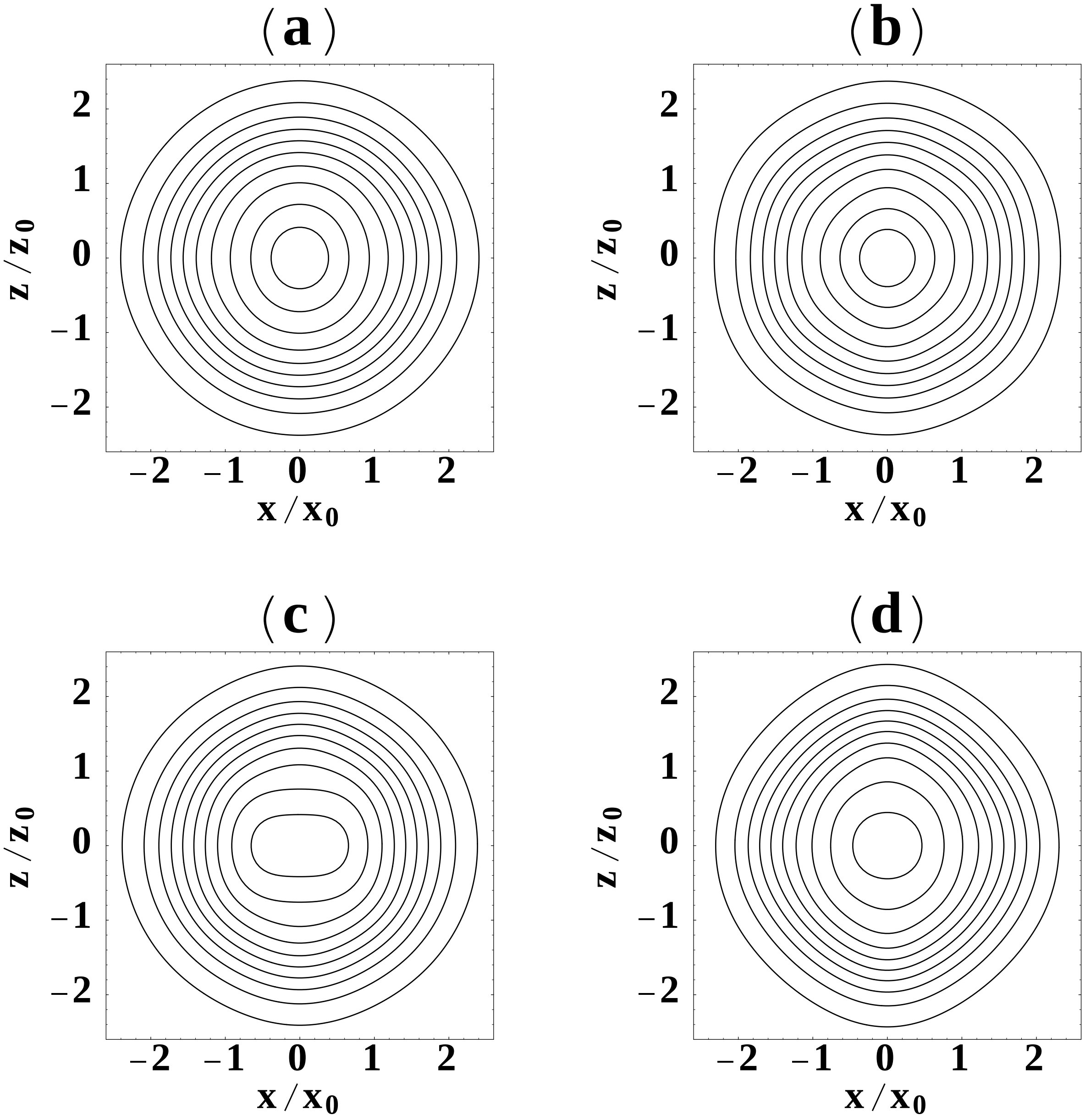

Fig. 5

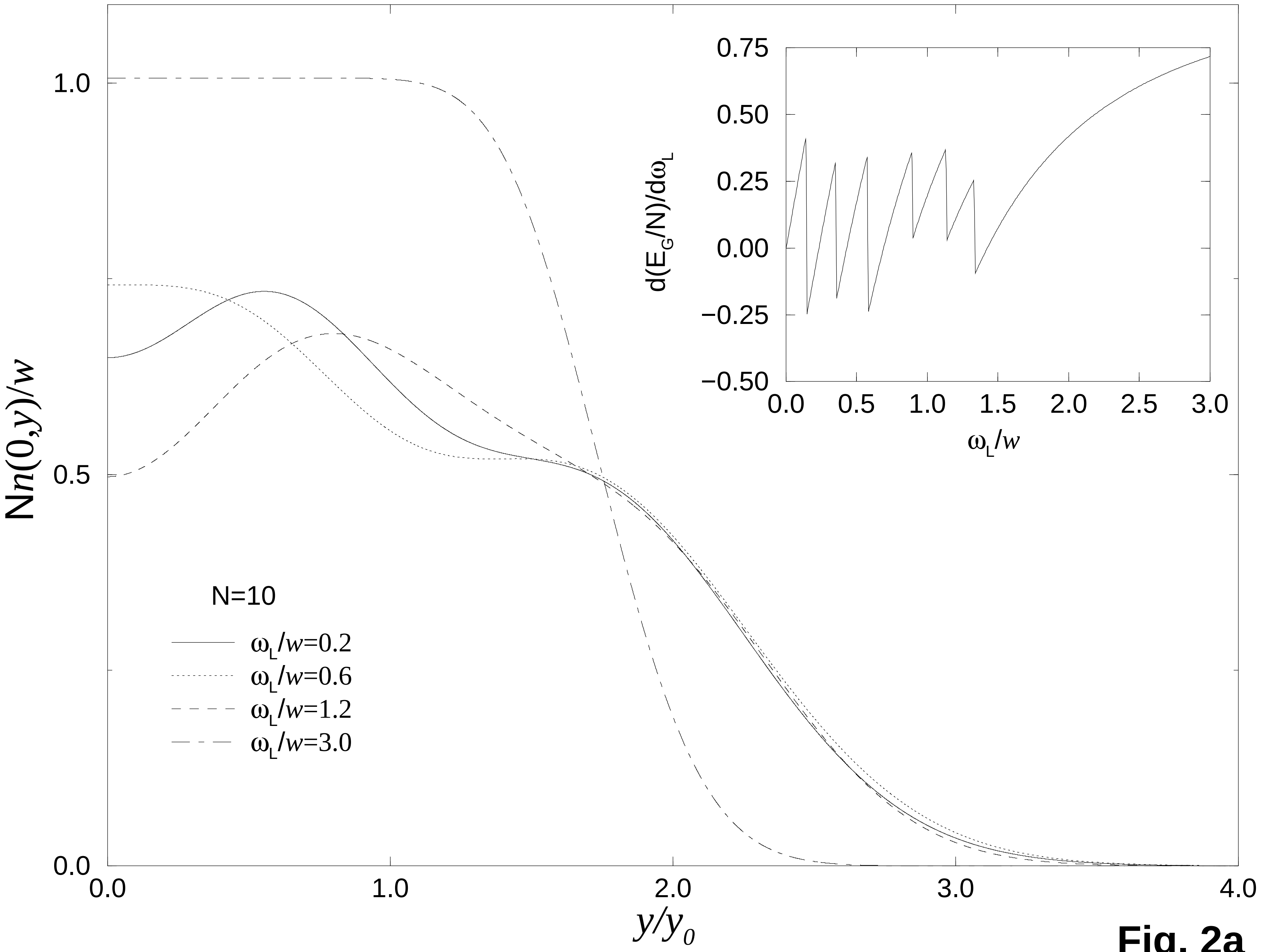

N*n*(0,*y*)/*w*
y/*y*0
1.0
0.5
0.0
0.0
1.0
2.0
3.0
4.0
N=10
ωL/w=0.2
ωL/w=0.6
ωL/w=1.2
ωL/w=3.0
d(EG/N)/dωL
ωL/w
0.75
0.50
0.25
0.00
−0.25
−0.50
0.0
0.5
1.0
1.5
2.0
2.5
3.0

Fig. 2a

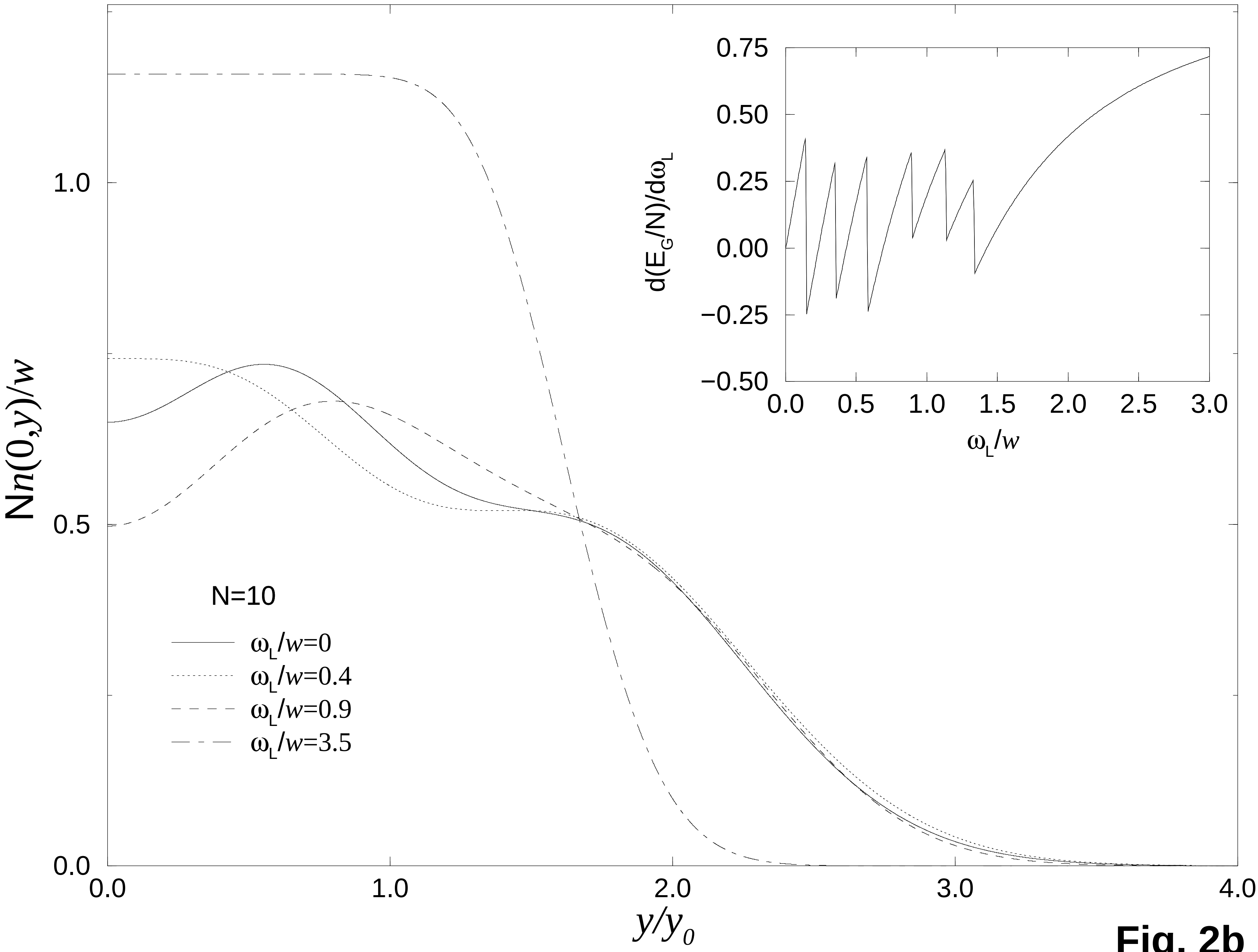

0.75
0.50
0.25
0.00
−0.25
−0.50
d(E_G/N)/dω_L
0.0
0.5
1.0
1.5
2.0
2.5
3.0
ω_L/w
1.0
0.5
0.0
Nn(0,y)/w
N=10
ω_L/w=0
ω_L/w=0.4
ω_L/w=0.9
ω_L/w=3.5
0.0
1.0
2.0
3.0
4.0
y/y_0

Fig. 2b

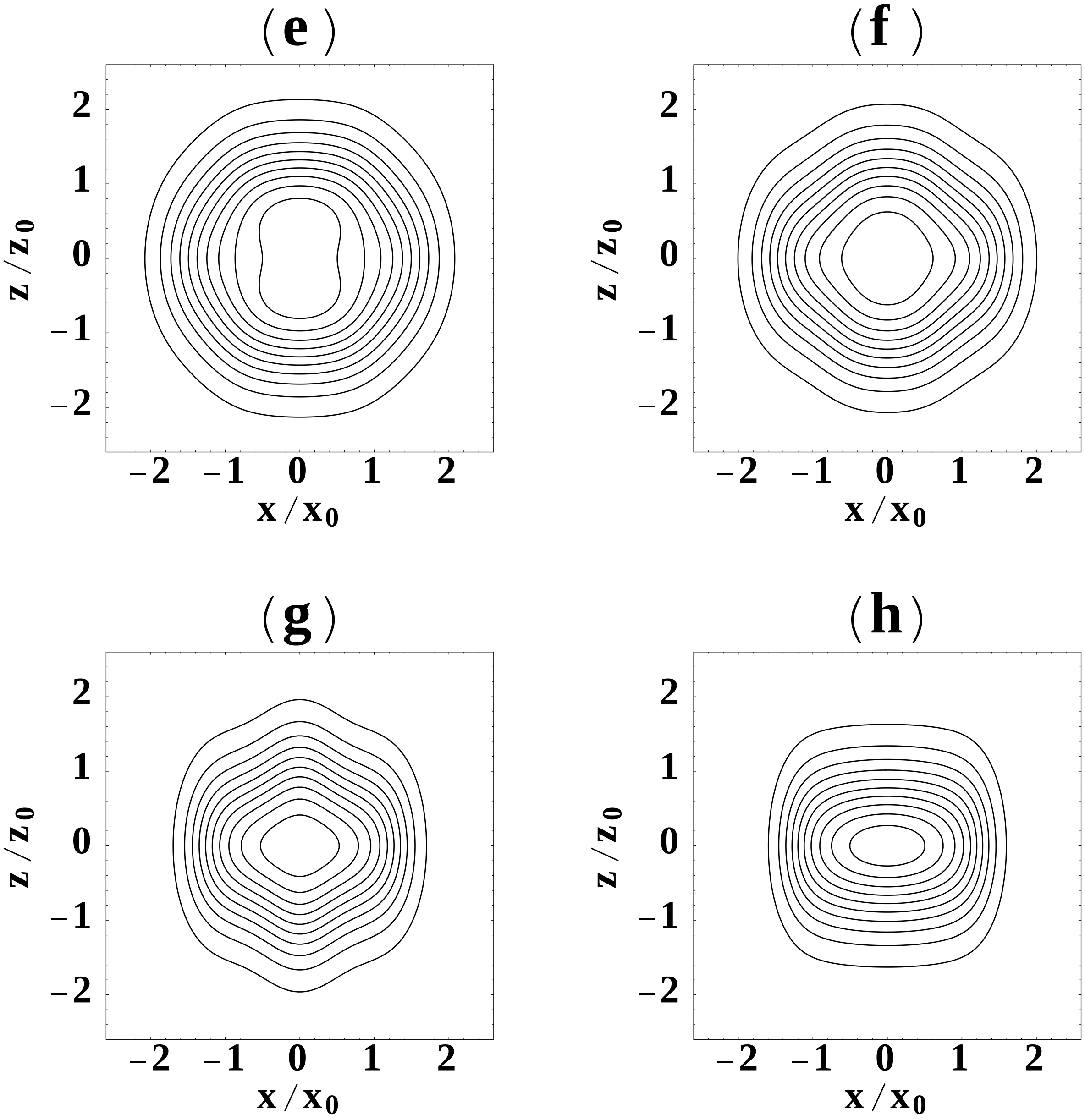

Fig. 5

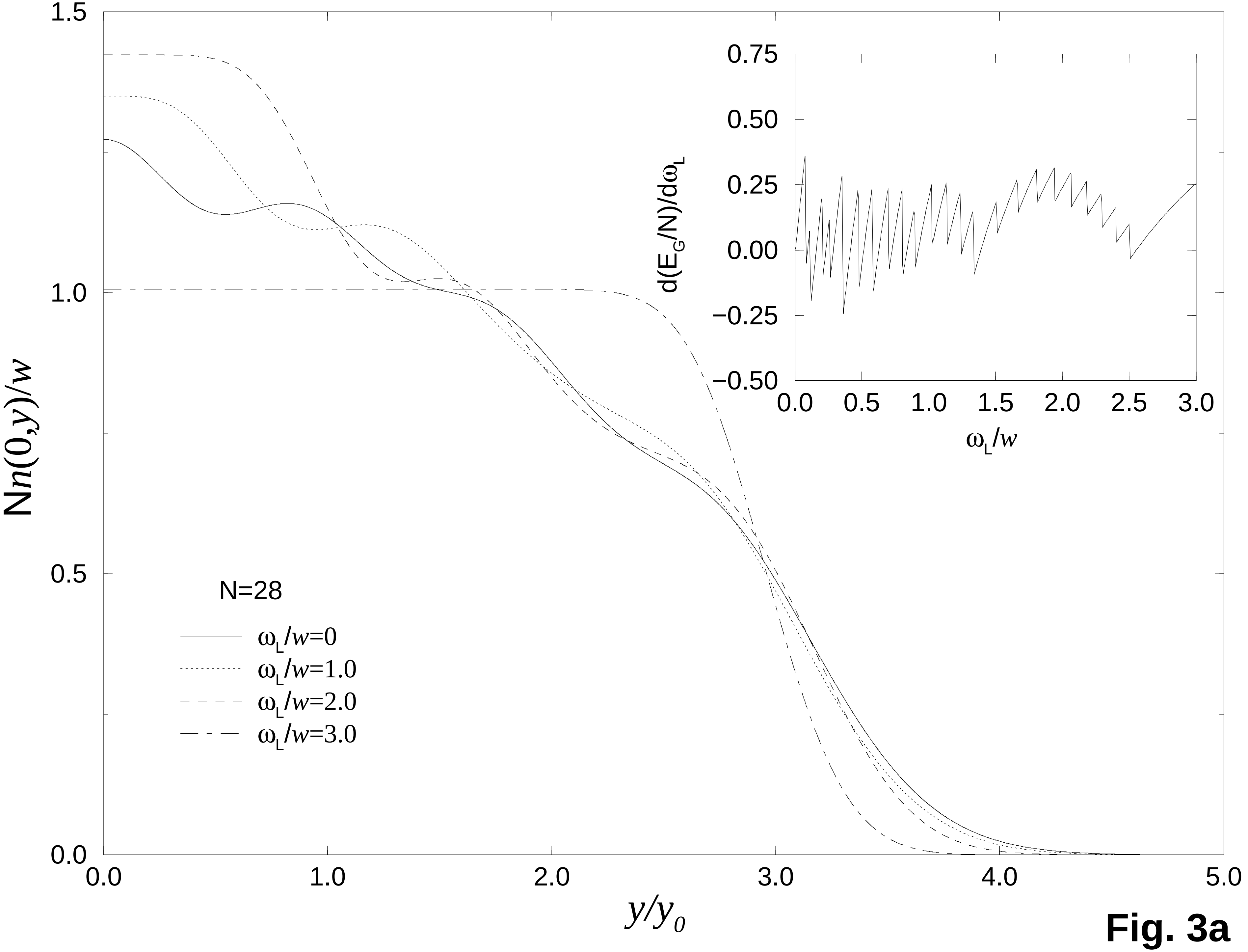
1.5
1.0
0.5
0.0
0.0
1.0
2.0
3.0
4.0
5.0
$Nn(0,y)/w$
y/y_0
N=28
$\omega_L/w=0$
$\omega_L/w=1.0$
$\omega_L/w=2.0$
$\omega_L/w=3.0$
0.75
0.50
0.25
0.00
−0.25
−0.50
0.0
0.5
1.0
1.5
2.0
2.5
3.0
$d(E_G/N)/d\omega_L$
ω_L/w

Fig. 3a

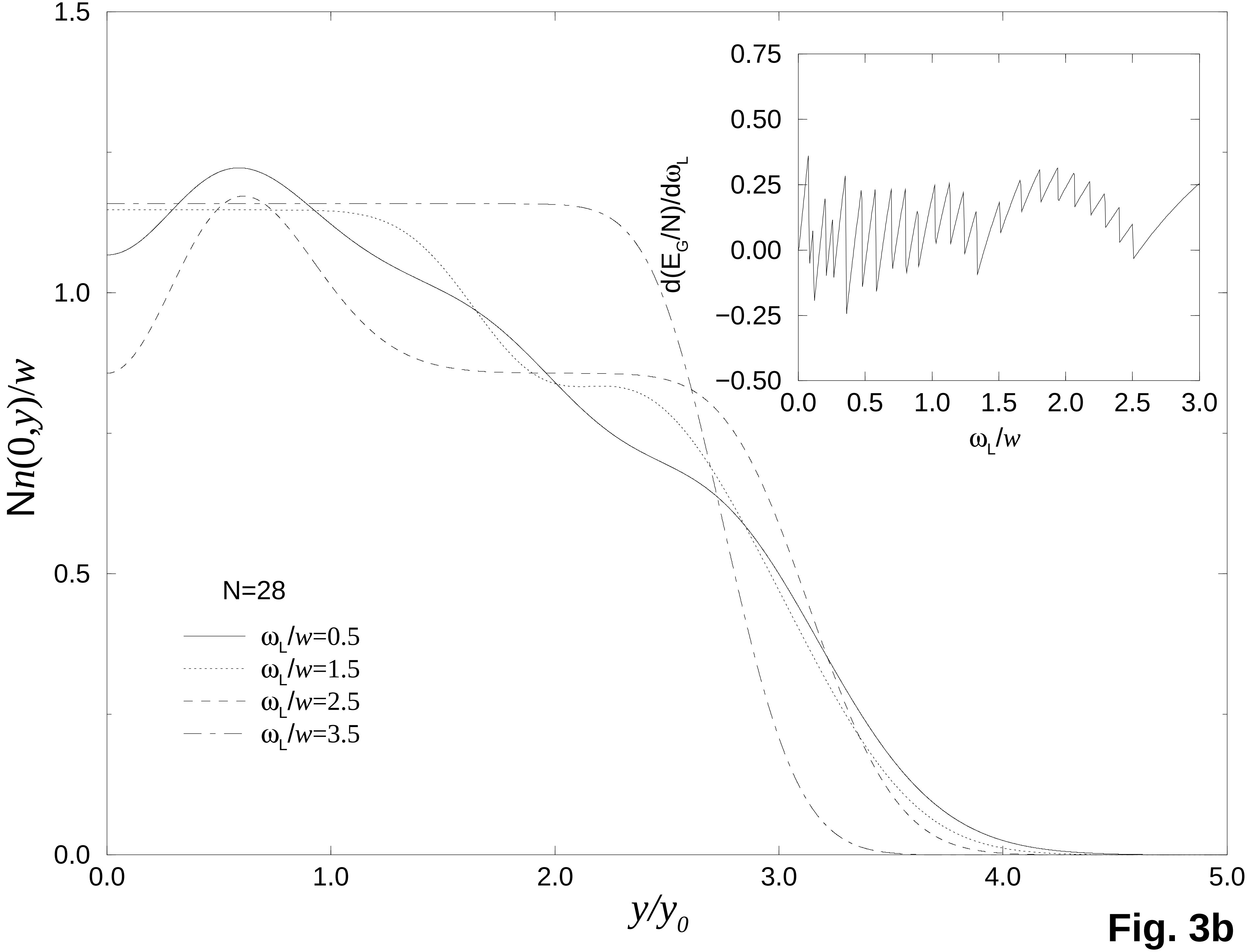

1.5
1.0
0.5
0.0
0.0
1.0
2.0
3.0
4.0
5.0
Nn(0,y)/w
y/y0
N=28
ωL/w=0.5
ωL/w=1.5
ωL/w=2.5
ωL/w=3.5
0.75
0.50
0.25
0.00
−0.25
−0.50
0.0
0.5
1.0
1.5
2.0
2.5
3.0
d(EG/N)/dωL
ωL/w

Fig. 3b

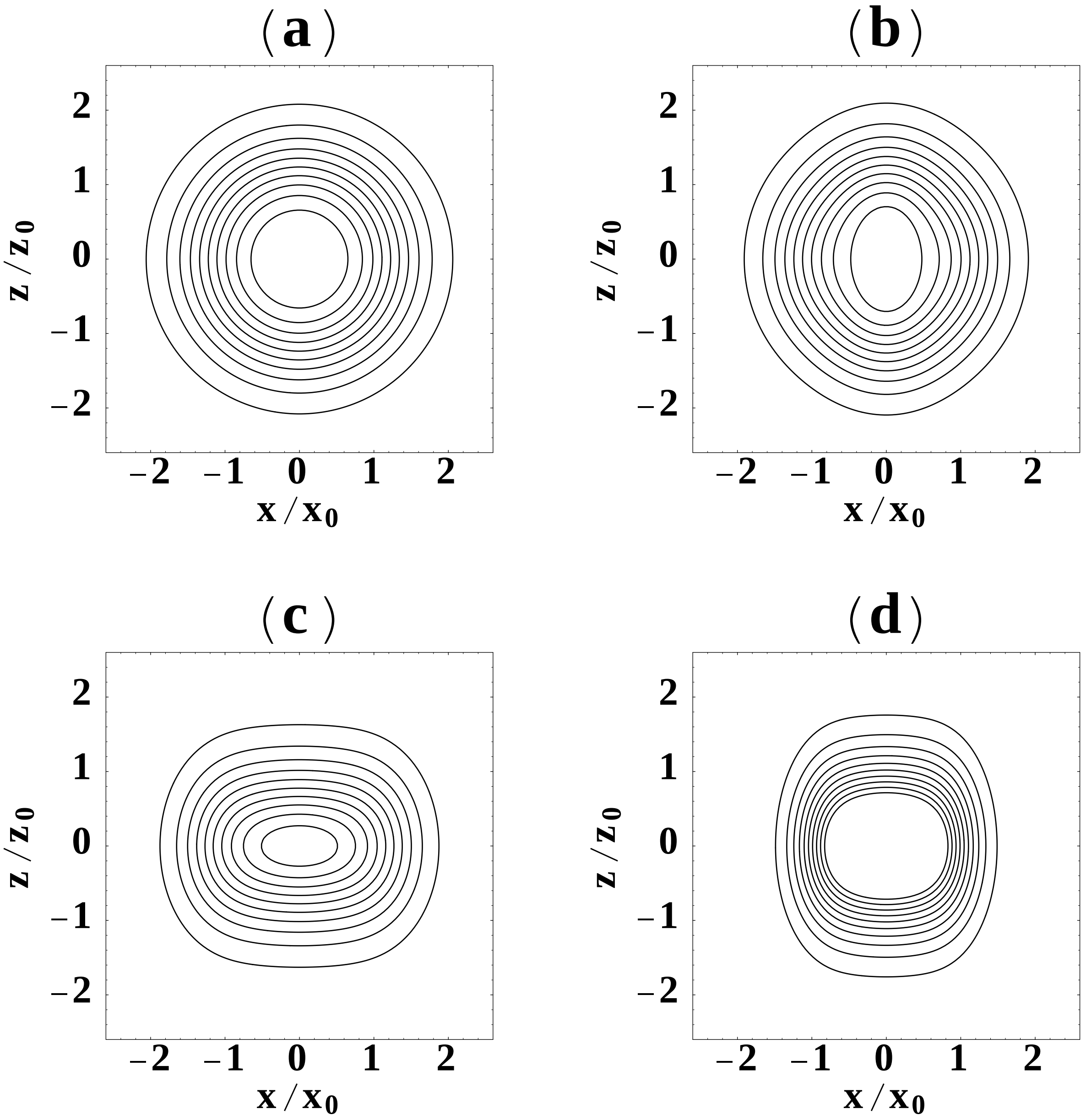

Fig. 4